Multiple Scattered Radiation Emerging from Continental Haze Layers.

2: Ellipticity and Direction of Polarization

By

Gilbert N. Plass, George W. Kattawar, and Stephen J. Hitzfelder
Department of Physics
Texas A&M University
College Station, Texas 77843

Report No. 19

The research described in this report was

funded by the

National Aeronautics and Space Administration

Contract No. NGR 44-001-117

Department of Physics
Texas A&M University
College Station, Texas 77843

August 11, 1975

A paper based on the material in this report has been submitted to Applied Optics.

Multiple Scattered Radiation Emerging from Continental Haze Layers.

2: Ellipticity and Direction of Polarization

By Gilbert N. Plass, George W. Kattawar, and Stephen J. Hitzfelder

ABSTRACT

The ellipticity and the direction of polarization are calculated for radiation that has undergone multiple scattering from plane parallel layers. Both the radiation emerging from the top of the layer and that transmitted through the bottom are considered. Two different phase functions are used for the scattering layer: Rayleigh and haze L. The direction of polarization of the reflected radiation shows little variation as the optical depth of the layer increases, while there is a much larger variation for the transmitted radiation. When the optical thickness is small, the direction of polarization for haze L varies rapidly with zenith angle near those angles at which the single scattered polarization is zero. The ellipticity of the radiation from haze L layers increases at first in direct proportion to the optical thickness of the layer. In general the ellipticity of the transmitted radiation is considerably greater than that of the reflected because of the greater average number of photon collisions in the former case. When the ellipticity is small, it is shown that the product of the polarization and the ellipticity is closely equal to $-V/2I$, where I and V are the first and fourth components of the Stokes vector.

The authors are with the Physics Department, Texas A&M University, College Station, Texas 77843.

I. Introduction

The radiation scattered by a planetary atmosphere is polarized even though the incoming solar radiation is essentially unpolarized. In the first part of this article[1] (referred to hereafter as I) we have discussed the degree of polarization together with the neutral points for photons emerging from the top and bottom of a homogeneous layer scattering either according to a Rayleigh or a haze L phase matrix. The dependence of the polarization on the optical thickness of the layer and the solar zenith angle has been discussed in I.

Two other important parameters of the radiation field, the direction of the polarization and the ellipticity, are presented in this, the second part of this article. These results were obtained at the same time and by the same matrix operator method discussed in I. They are presented separately for clarity and convenience of presentation.

II. Direction of Polarization

The angle χ which the direction of polarization (maximum intensity component) makes with the direction of the meridian plane containing the final photon direction is given by

$$\tan 2\chi = U/Q, \tag{1}$$

where U and Q are two of the four components of the Stokes vector (I,Q, U,V). The range $0° < \chi < 180°$ has been chosen for the principal value of χ. The values of 0° and 180° have equivalent physical meanings. Thus when there is a continuous rotation of the direction of polarization as μ increases and χ passes through 0° or 180°, this would be represented on a figure giving χ as a function of μ by a curve which goes off the top of the figure (180°) and reappears at the bottom (0°), or vice versa.

The direction of polarization χ of the photons scattered by a Rayleigh phase matrix from a layer of optical thickness τ is shown in Fig. 1. Curves are given for both the photons reflected upward out of the top of the layer and for those transmitted through the layer and passing through its bottom surface in a downward direction. The curves in Fig. 1 are for the case when the cosine of the solar zenith angle $\mu_o = 0.85332$ (31.43°), the surface albedo $A = 0$, and the azimuthal angle $\phi = 30°$ and 150°. The abscissa is the cosine of the nadir (for reflected photons) or zenith (for transmitted photons) angle of observation, μ. The solar horizon is at the left of the figure, the antisolar horizon is at the right, and the nadir or zenith is at the center.

For the reflected radiation and single scattered photons ($\tau = 0$), $\chi = 73°$ at the solar horizon and changes only a small amount as μ increases; near the nadir χ decreases to 60°, a value that it must have as the nadir is approached from the $\phi = 30°$ side for any optical thickness. The corresponding value of χ is 120° as the nadir is approached from the $\phi = 150°$ side. As the angle of observation decreases from the nadir to the antisolar horizon, χ varies rapidly at first and has the value 73° on the antisolar horizon. The range of χ is taken as 0° to 180°; thus, if χ is increasing on the graph and reaches the value 180°, the curve terminates at the top of the graph and reappears at the bottom at 0°. This is not a real discontinuity in the motion of the direction of polarization, which moves in a perfectly continuous manner; only the graphical representation has this jump. A better representation is obtained if one imagines the top and bottom of the graph joined together to form a cylinder. Then there is no discontinuity in the curves at such a point. The variation of χ with τ is small for the reflected photons. The curve for $\tau = 4$ is a limiting curve which is the same for all larger values of

τ on the scale of the graph.

The values of χ shown in Fig. 1 for the transmitted photons exhibit more variation as the optical depth increases than was the case for the reflected photons. When the optical depth is very small, χ decreases from a value of 73° at the solar horizon to 0° as ϕ increases. Because of the chosen range of χ, the value then jumps to 180° (as already explained) and approaches 120° as the zenith is approached from this side. From the other side of the zenith (ϕ = 150°) χ starts at 60°, increases to about 75°, and decreases to 73° at the anti-solar horizon. The curve for the photons transmitted through a layer of optical depth $\tau = 4$ shows variations of up to 20° from the curve from small τ. However, the curve for $\tau = 16$ has an entirely different form. The direction of polarization χ has the value 90° everywhere except over a small region very near the zenith. The reason for this is that the photons transmitted through the diffusion region for layers of large optical depth have lost all memory of the original solar direction.

The direction of polarization of radiation scattered by a Rayleigh phase matrix for a low solar elevation, $\mu_o = 0.18817$, is shown in Fig. 2 when ϕ = 30° and 150°. The curve for $\tau = 4$ for the transmitted photons shows an interesting transition between the curves typical of smaller and larger values of τ.

The variation of χ for radiation scattered by the haze L phase matrix is shown in Fig. 3. The variation is obviously more complicated than that for the Rayleigh phase matrix. There is little variation of χ as the optical depth increases for the radiation reflected from the top of the haze L layer. On the other hand τ depends strongly on the optical thickness of the layer for the radiation transmitted through a haze L layer of optical thickness τ. When $\tau = 0$ (single scattered photons), the variation of χ in the ϕ = 30° half plane is worthy of comment. The value of

χ is 150° at the zenith. As μ decreases in the $\phi = 30°$ half plane, χ decreases discontinuously by 90° as μ passes through the value 0.9927 ($\theta = 6.93°$). Kattawar and Plass[2] have discussed the discontinuity which occurs whenever M^- (the second independent element of the scattering matrix occurring in positions S_{12} and S_{21} when the Stokes vector is chosen with the components I, Q, U, V) changes sign. For haze L the value of M^- changes sign at scattering angles (Θ) of 3.53° and 25.63°. When $M^- = 0$, the scattered radiation is unpolarized, and the value of χ is indeterminate (see Fig. 18 of I for the zeros of the single scattered polarization). Thus there is no physical difficulty in determining the direction of polarization for any given scattering angle.

When $\tau = 0$, $\mu = 0.9927$ and $\phi = 30°$, the scattering angle $\Theta = 25.63°$ and $M^- = 0$; thus the value of χ decreases by 90° as μ passes through this value. As μ decreases further in the $\phi = 30°$ half plane, the scattering angle decreases to 15.1° and then increases again passing through the value 25.63° again when $\mu = 0.6582$ ($\theta = 48.83°$). Once more χ decreases discontinuously by 90°. As μ continues to decrease, χ decreases continuously until the horizon is reached.

When $\tau > 0$, there is no actual discontinuity in the curve for χ at the points just discussed. For example, the curve for $\tau = 1$ follows fairly closely the $\tau = 0$ curve. There is a rapid change in the value of χ near $\mu = 0.6582$, but no actual discontinuity. When $\tau = 8$, the curve is quite different from those for smaller optical thicknesses. When $\tau = 16$, χ decreases slightly from the initial value of 150° at the zenith as μ decreases ($\phi = 30°$) and then increases to a value of 180° at the horizon. Unfortunately the computer run was terminated at this value of the optical thickness. Presumably χ would have the value of 180° (or the equivalent 0°) for all values of μ except at the zenith for large optical thicknesses.

The variation of χ in the $\phi = 90°$ plane is shown in Fig. 4 when $\mu_o = 0.85332$ (31.43°). There is little variation with optical depth for the reflected photons, but considerably more variation for the transmitted photons.

The variation of χ for both the reflected and transmitted photons from haze L layers of various optical thicknesses is given in Fig. 5 for $\mu_o = 0.188166$ (79.15°). Once again there is little variation with optical thicknesses for the reflected photons, but considerably more for the transmitted. There are no discontinuities in the χ curves, since the scattering angle never becomes as small as 25.63° in this case.

III. Ellipticity

The ellipticity of the radiation, E, is defined as the ratio b/a, where a and b are respectively proportional to the major and minor axes of the ellipse described by the end point of the electric vector. This can be written in terms of the Stokes parameters I, Q, U, V as

$$E = - \tan \{\frac{1}{2} \sin^{-1} [V(Q^2 + U^2 + V^2)^{-\frac{1}{2}}]\} \tag{2}$$

and

$$E \simeq - \frac{1}{2} V(Q^2 \; U^2 + V^2)^{-\frac{1}{2}}. \tag{3}$$

In almost all practical cases the ellipticity is small compared to unity and the approximate expression is sufficiently accurate.

There is an interesting relationship between the polarization and the ellipticity. The polarization is defined as

$$P = (Q^2 + U^2 + V^2)^{\frac{1}{2}}/I. \tag{4}$$

Thus

$$E = - \tan [\frac{1}{2} \sin^{-1}(V/PI)], \tag{5}$$

$$E \simeq -V/2PI \tag{6}$$

or

$$2\,I\,P\,E \simeq -V \tag{7}$$

This simple approximate equation is usually quite accurate whenever $E \ll 1$. For haze L, Eq. (7) is accurate to six or seven significant figures for most angles. These equations remind us that the ellipticity is zero whenever V is zero (which is always the case for Rayleigh scattering). The quantity V is also zero for any spherical polydispersion in the principal plane.

The polarization in general tends to be large in a region where the ellipticity is small, as is shown by Eq. (7), and vice versa. It has been claimed that the calculated values of the ellipticity in the region where the polarization is small are uncertain due to truncation errors. We believe that our values are real from various tests which we have performed including varying the number of significant figures. All of our computed values of P, χ (the angle of polarization), and E are very well behaved in the regions where E is small.

The phase matrix for spherical particles has a zero entry in the fourth row and first column; thus incident unpolarized radiation cannot create a circular component from a single scattering. The photon must be scattered several times to be elliptically polarized. The ellipticity is shown in Fig. 6 for the reflected photons from a haze L layer when $\mu_o = 0.85332$ (31.43°) and $\phi = 30°$ and 150°. A study of all the numerical results (including others not shown in the figure) shows that the ellipticity increases linearly with the optical thickness (τ) for small values of τ. The ellipticity changes sign with V and thus is zero at certain particular angles. The absolute value of the ellipticity is plotted on a logarithmic scale in all the figures in this article.

The nadir angle at which the ellipticity is zero is given for certain solar angles in Table 1. In the $\phi = 30°$ half plane, for example, there is one neutral point which does not change greatly with the optical thickness of the scattering layer for $\tau \leq 1$. When $\tau = 2$, there is no neutral point. On the other hand there are two neutral points when $\tau = 4$ (not shown in the figure). There is one neutral point for $\tau \geq 8$ near $\theta = 16°$. The behavior of the neutral points for the ellipticity is just as complicated as those for the polarization.

The ellipticity of the reflected radiation does not increase appreciably with τ for $\tau > 0.25$ and has typical values of about 10^{-3} away from neutral points. There may be zero, one, or two of these neutral points in each half plane in addition to the neutral point that always exists at the nadir.

The ellipticity of the photons transmitted through a haze L layer of optical thickness τ is given in Fig. 7 for the same solar zenith angle. Again the results (including others not shown in the figure) show that the ellipticity increases linearly with τ for small values of τ. A few comments follow on some of the many complicated features shown in Fig. 7. A very sharp peak in the ellipticity develops near $\mu = 0.66$ in the $\phi = 30°$ half plane which persists for optical thicknesses as large as unity. There are neutral points whose position is given in Table 1. The ellipticity continues to increase in many regions as τ increases up to $\tau = 8$ or 16. Values for the ellipticity between 10^{-2} and 0.13 develop in the $\phi = 30°$ half plane.

It is important to note that typical values for the ellipticity of the transmitted radiation for larger optical thicknesses are from one to two orders of magnitude larger than the corresponding values for the reflected radiation. The transmitted photons for the larger optical thicknesses undergo more multiple scattering than the reflected photons. The ellipticity increases in general with the number of scattering events, at least for relatively small numbers of such events.

The ellipticity is always zero in the principal plane. The values when $\phi = 90°$ are shown in Fig. 8 as an example of the variation in another plane. The neutral points are given in Table 1. The other features already pointed out can also be seen here.

The ellipticity when the sun is near the horizon ($\mu_o = 0.188166$, $\theta = 79.15$) is given in Figs. 9, 10, and 11 for the reflected and transmitted radiation in the $\phi = 30°$ and $120°$ and the $\phi = 90°$ half planes. The linear dependence of the ellipticity on τ when τ is small is clearly seen in these figures. The neutral points are given in Table 1. Their dependence on is especially interesting in the $\phi = 150°$ half plane for the transmitted photons. There is one neutral point when $\tau \leq 0.0625$; two when $\tau = 0.25$; none when $\tau = 1$ and 2; and one when $\tau \geq 4$.

IV. Conclusions

The complicated variation of the direction of polarization and of the ellipticity of the radiation scattered from the top and transmitted through the bottom of Rayleigh and haze L layers has been illustrated. The direction of polarization of the reflected radiation shows only relatively small variations as the optical depth of the layer is changed; on the other hand the variations are much larger for the transmitted radiation. The direction of polarization of the single scattered transmitted radiation for haze L may undergo a discontinuous change of 90° at those scattering angles where the polarization is zero. When the radiation is transmitted through a finite layer, the corresponding variation of the direction of polarization is rapid as the angle of view passes through the angle at which there is a discontinuity for single scattering (until the optical thickness becomes large).

The ellipticity of the radiation reflected by and transmitted through haze L layers increases at first in direct proportion to the optical thickness (τ) of the layer as τ increases from zero. In general the ellipticity of the transmitted radiation is considerably greater than that of the reflected because of the greater average number of photon collisions in the former case. When the ellipticity is small compared to unity, the relation $V = - 2 I P E$ is very accurate, where I and V are the first and fourth components respectively of the Stokes vector, P is the polarization, and E is the ellipticity.

This work was supported in part by Grant No. NGR 44-001-117 from the National Aeronautics and Space Administration. Acknowledgement is made to the National Center for Atmospheric Research, which is sponsored by the National Science Foundation, for computer time used in this research.

References

1. Kattawar, G. W., G. N. Plass, and S. J. Hitzfelder, Appl. Opt. xx, xxx (1976).

2. Kattawar, G. W., and G. N. Plass, Appl. Opt. 11, 2851 (1972).

Table 1.

Zenith or nadir angle at which ellipticity is zero

Solar Zenith Angle	Reflected (R) or Transmitted (T)	Optical Thickness	$\phi = 30°$	$\phi = 90°$	$\phi = 150°$
31.43°	R	0.00195	79.9°	72.3°	76.4°
		0.00781	79.7°	72.1°	76.2°
		0.0625	78.7°	70.7°	75.1°
		0.25	76.9°	67.9°	72.4°
		1	76.5°	64.4°	67.0°
		2	None	63.8°	62.6°
		4	6.3°; 13.3°	64.0°	58.7°
		8	16.3°	64.0°	58.0°
		16	15.8°	64.0°	58.0°
31.43°	T	0.00195	75.5°	72.2°	78.2°
		0.00781	77.3°	71.9°	78.1°
		0.0625	76.2°	70.4°	77.1°
		0.25	73.4°	67.2°	75.0°
		1	64.9°	62.4°	72.8°; 86.6°
		2	20.8°	56.7°; 87.1°	None
		4	None	69.9°	44.1°
		8	None	68.9°	58.2°
		16	None	75.3°	38.3°
79.15°	R	0.00195	None	64.3°	80.7°
		0.00781	None	63.0°	80.7°
		0.0625	None	62.4°	80.5°
		0.25	None	62.2°	79.4°
		1	None	63.4°	76.4°
		2	None	63.9°	75.2°
		4	None	64.0°	74.6°
		8	None	64.0°	74.6°
		16	None	64.0°	74.6°
79.15°	T	0.00195	88.9°	64.1°	77.5°
		0.00781	88.5°	64.0°	77.3°
		0.0625	85.7°	63.1°	75.9°

Table 1 (cont.)

Solar Zenith Angle	Reflected (R) or Transmitted (T)	Optical Thickness	$\phi = 30°$	$\phi = 90°$	$\phi = 150°$
		0.25	80.2°	61.0°	71.2°; 85.4°
		1	63.1°	54.3°	None
		2	38.3°	42.2°; 79.5°	None
		4	None	68.0°	26.0°
		8	None	68.8°	19.6°
		16	None	76.8°	9.9°

CAPTIONS FOR FIGURES

Fig. 1. Direction of polarization (χ) as a function of cosine (μ) of nadir angle (for reflected photons) and of zenith angle (for transmitted photons). The cosine of the solar zenith angle, $\mu_o = 0.85332$, the surface albedo, $A = 0$, and the azimuthal angle, $\phi = 30°$ for the left half of the figure and $\phi = 150°$ for the right half. Curves are given for various values of the optical thickness τ of the Rayleigh scattering layer.

Fig. 2. Direction of polarization for $\mu_o = 0.18817$, $A = 0$, $\phi = 30°$ and $150°$, and Rayleigh scattering. See caption to Fig. 1.

Fig. 3. Direction of polarization for $\mu_o = 0.85332$, $A = 0$, $\phi = 30°$ and $150°$, and haze L scattering. See caption to Fig. 1.

Fig. 4. Direction of polarization for $\mu_o = 0.85332$, $A = 0$, $\phi = 90°$, and haze L scattering. See caption to Fig. 1.

Fig. 5. Direction of polarization for $\mu_o = 0.188166$, $A = 0$, $\phi = 30°$ and $150°$, and haze L scattering. See caption to Fig. 1.

Fig. 6. Absolute value of ellipticity (E) as a function of cosine of nadir angle (μ) for $\mu_o = 0.85332$, $A = 0$, $\phi = 30°$ and $150°$ for photons reflected from a haze L scattering layer of optical thickness τ.

Fig. 7. Absolute value of ellipticity (E) as a function of cosine of zenith angle (μ) for $\mu_o = 0.85332$, $A = 0$, $\phi = 30°$ and $150°$ for photons transmitted through a haze L scattering layer of optical thickness τ.

Fig. 8. Absolute value of ellipticity (E) as a function of cosine of nadir or zenith angle (μ) for $\mu_o = 0.85332$, $A = 0$, $\phi = 90°$ for photons reflected from and transmitted through a haze L scattering layer of optical thickness τ.

Fig. 9. Absolute value of ellipticity (E) as a function of cosine of nadir angle (μ) for $\mu_o = 0.188166$, $A = 0$, $\phi = 30°$ and $150°$ for photons reflected from a haze L scattering layer of optical thickness τ.

Fig. 10. Absolute value of ellipticity (E) as a function of cosine of zenith angle (μ) for μ_o = 0.188166, A = 0, ϕ = 30° and 150° for photons transmitted through a haze L scattering layer of optical thickness τ.

Fig. 11. Absolute value of ellipticity (E) as a function of cosine of nadir or zenith angle (μ) for μ_o = 0.188166, A = 0°, ϕ = 90° for photons reflected from and transmitted through a haze L scattering layer of optical thickness τ.

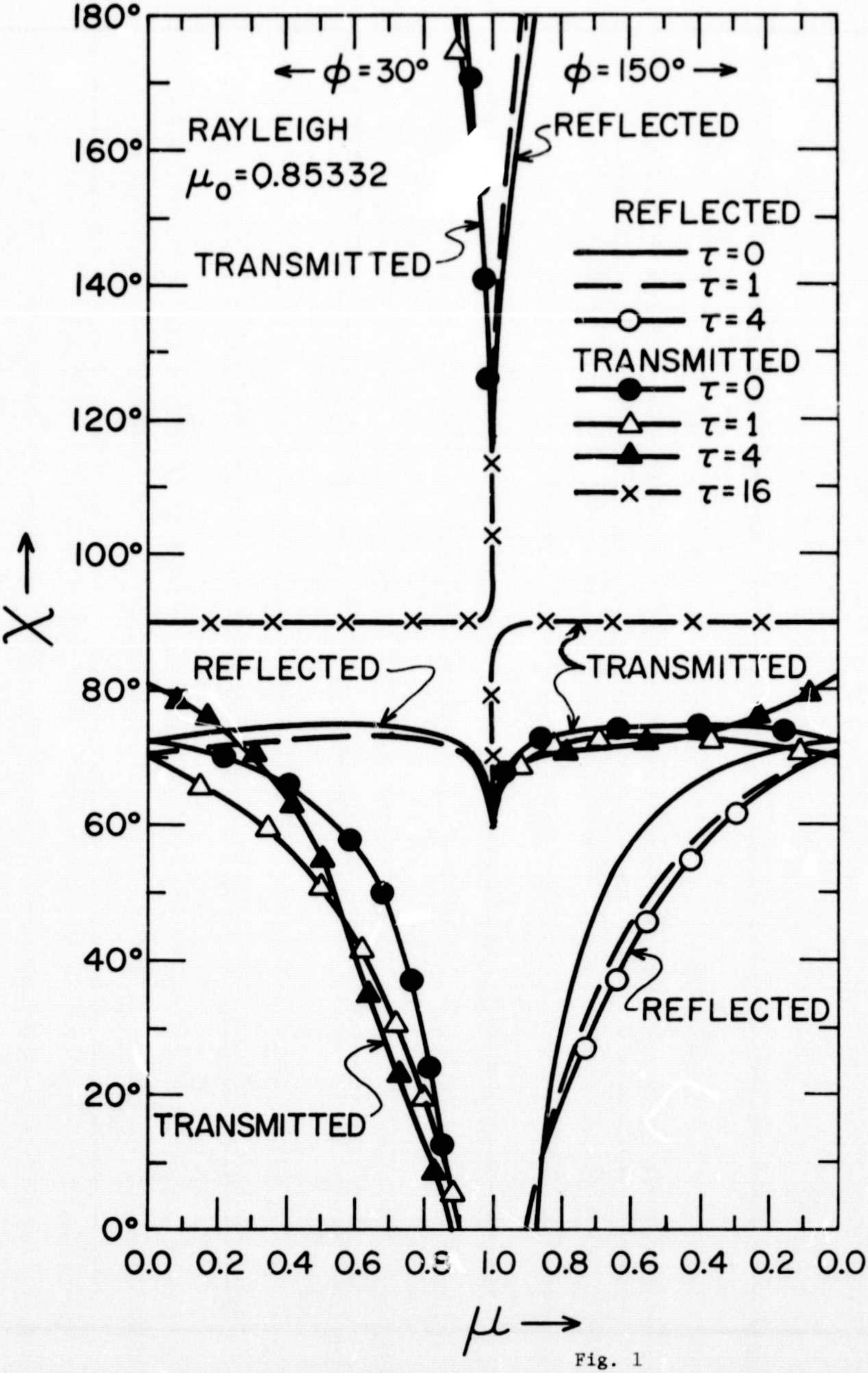
180°
160°
140°
120°
100°
80°
60°
40°
20°
0°
χ
← φ=30°
φ=150° →
RAYLEIGH
μ0=0.85332
REFLECTED
TRANSMITTED
REFLECTED
τ=0
τ=1
τ=4
TRANSMITTED
τ=0
τ=1
τ=4
τ=16
REFLECTED
TRANSMITTED
REFLECTED
TRANSMITTED
0.0 0.2 0.4 0.6 0.8 1.0 0.8 0.6 0.4 0.2 0.0
μ →

Fig. 1

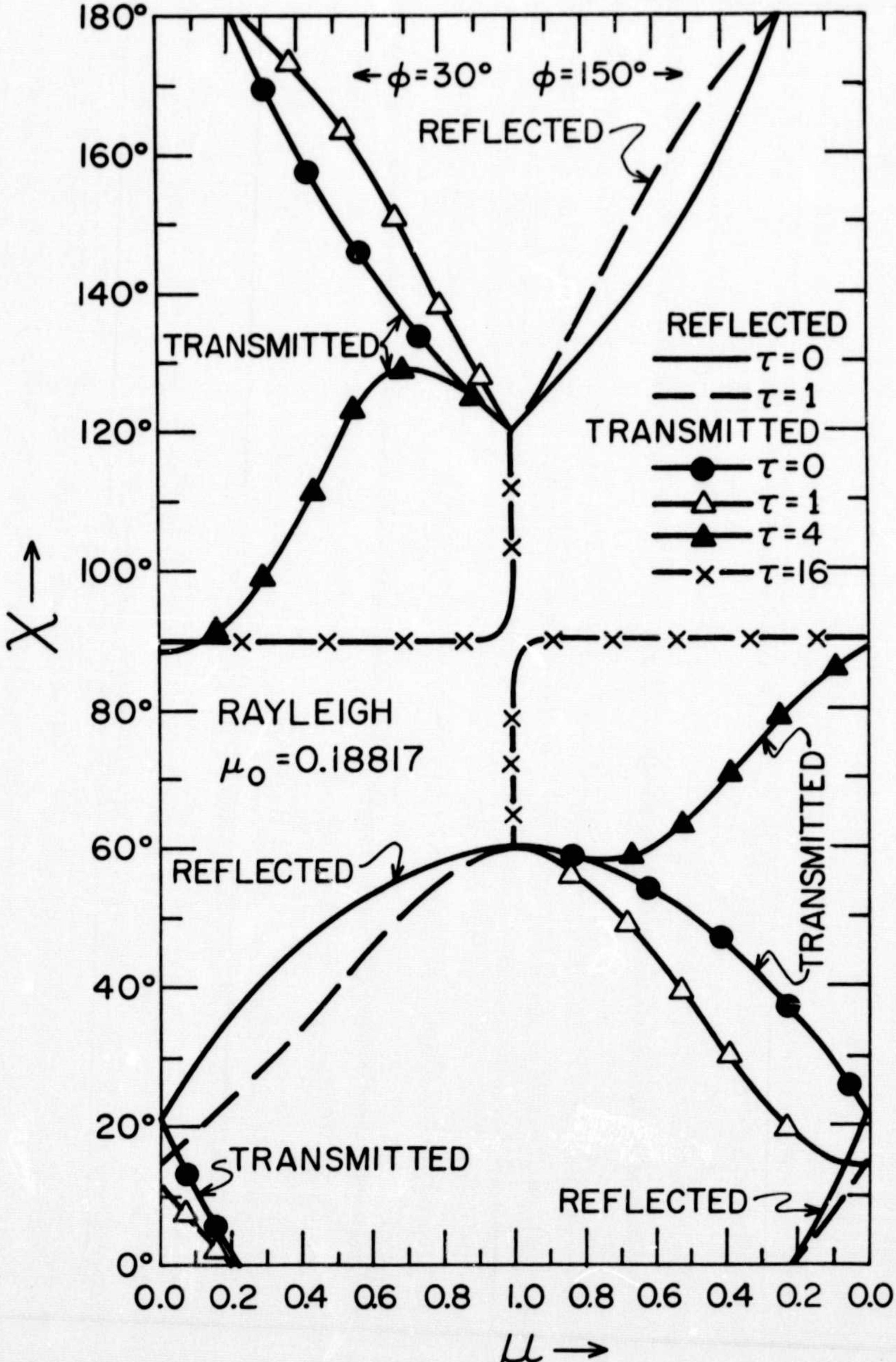

180°
160°
140°
120°
100°
80°
60°
40°
20°
0°
χ
←φ=30° φ=150°→
REFLECTED
TRANSMITTED
REFLECTED
τ=0
τ=1
TRANSMITTED
τ=0
τ=1
τ=4
τ=16
RAYLEIGH
μ0=0.18817
REFLECTED
TRANSMITTED
TRANSMITTED
REFLECTED
0.0 0.2 0.4 0.6 0.8 1.0 0.8 0.6 0.4 0.2 0.0
μ

Fig. 2

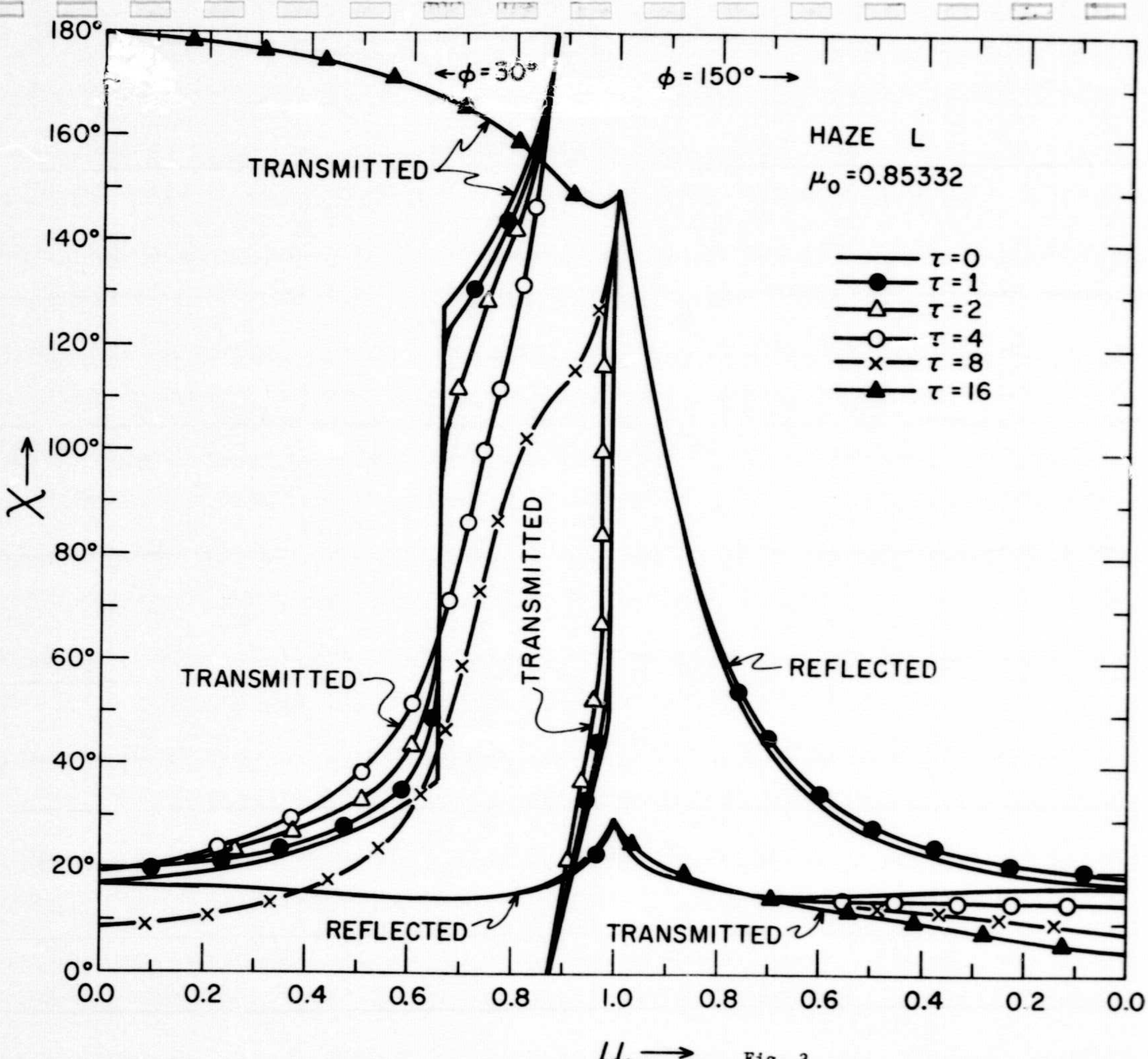

180°
160°
140°
120°
100°
80°
60°
40°
20°
0°
χ →
0.0
0.2
0.4
0.6
0.8
1.0
0.8
0.6
0.4
0.2
0.0
μ →
← φ = 30°
φ = 150° →
HAZE L
μ_0 =0.85332
τ = 0
τ = 1
τ = 2
τ = 4
τ = 8
τ = 16
TRANSMITTED
TRANSMITTED
TRANSMITTED
REFLECTED
REFLECTED
TRANSMITTED

Fig. 3

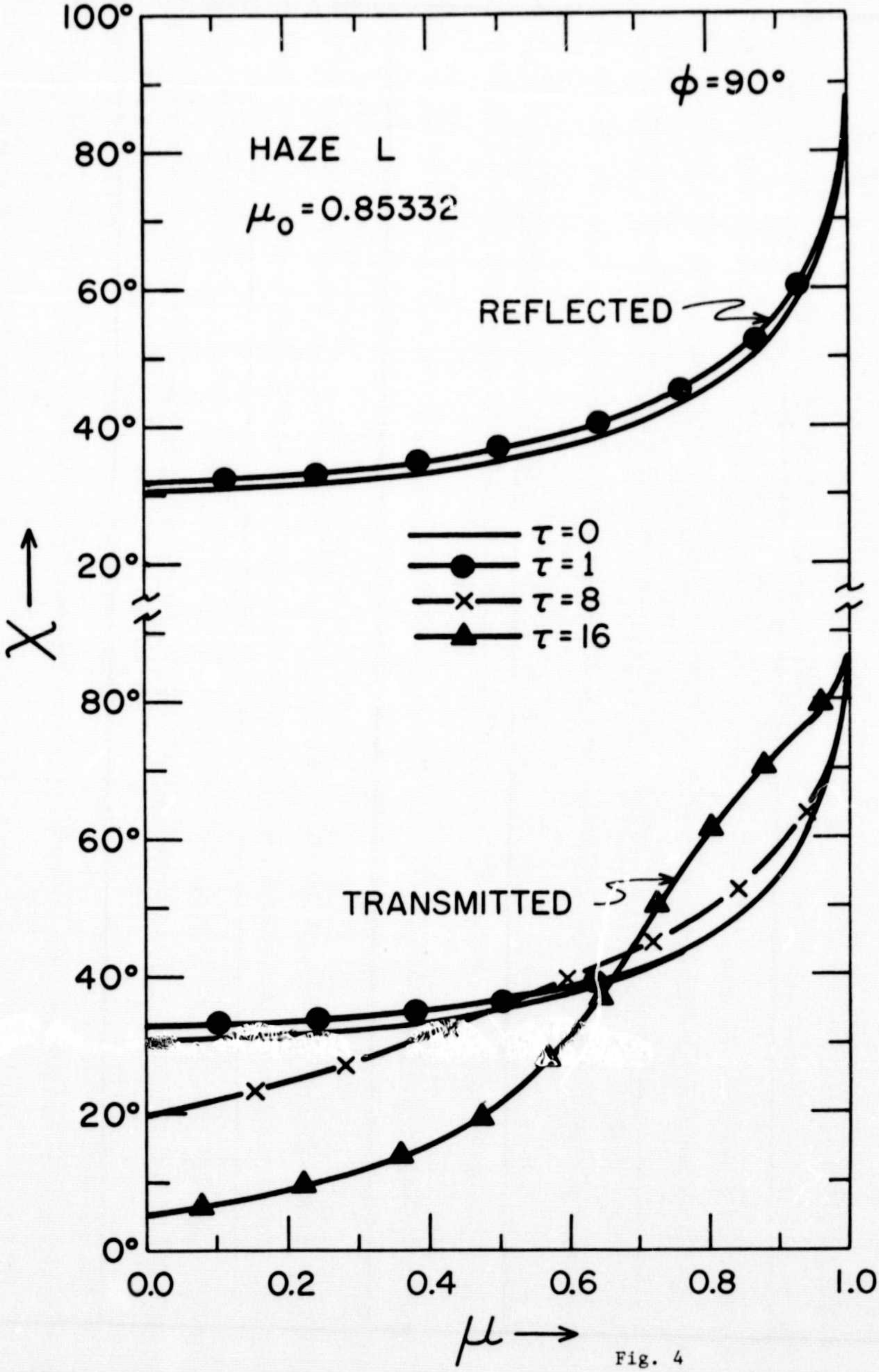

100°
80°
60°
40°
20°
0°
ϕ=90°
HAZE L
μ_0=0.85332
REFLECTED
TRANSMITTED
τ=0
τ=1
τ=8
τ=16
χ
0.0
0.2
0.4
0.6
0.8
1.0
μ

Fig. 4

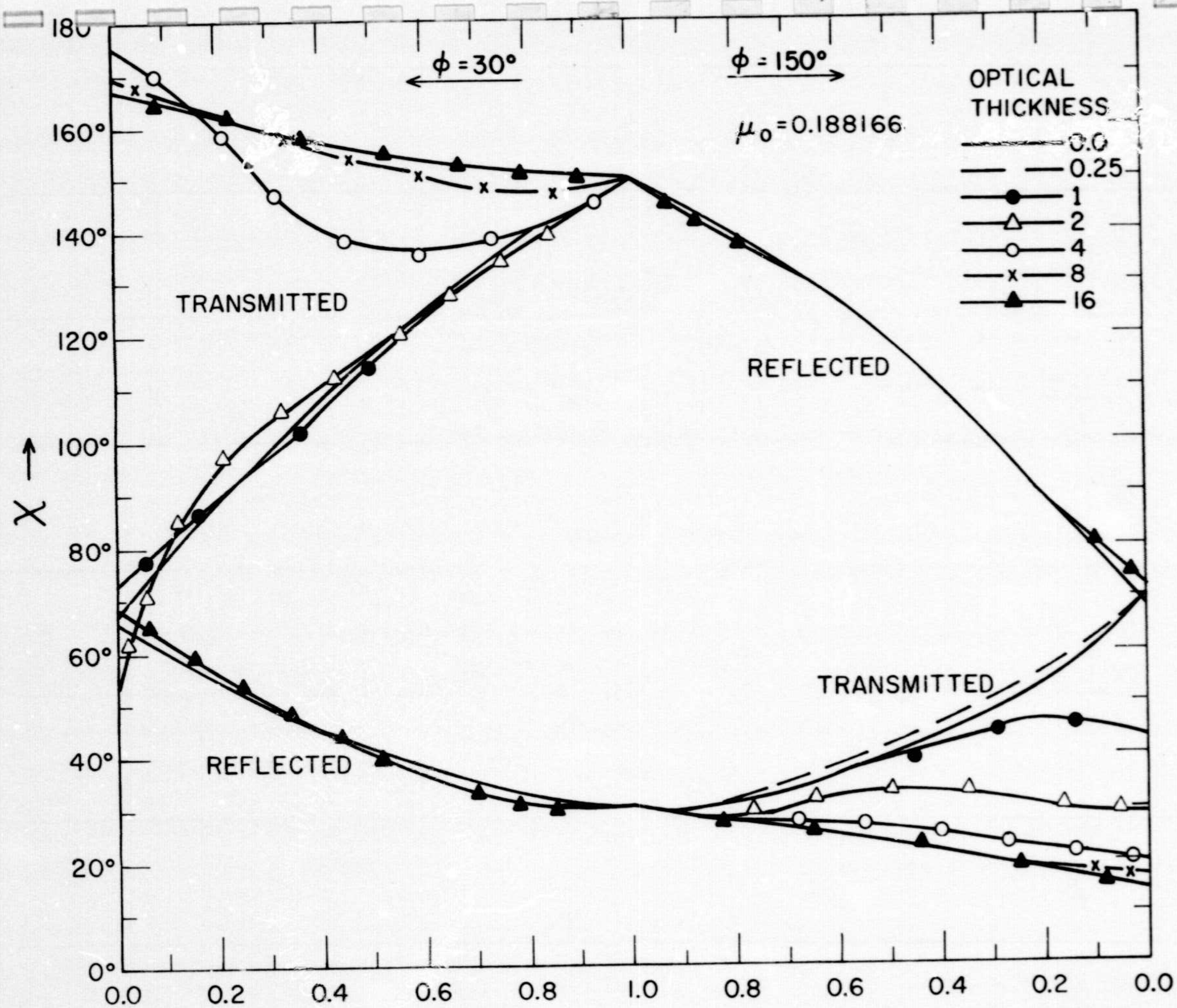

180
160°
140°
120°
100°
80°
60°
40°
20°
0°
χ →
φ = 30°
φ = 150°
μ₀ = 0.188166
OPTICAL
THICKNESS
0.0
0.25
1
2
4
8
16
TRANSMITTED
REFLECTED
REFLECTED
TRANSMITTED
0.0
0.2
0.4
0.6
0.8
1.0
0.8
0.6
0.4
0.2
0.0
μ →

Fig. 5

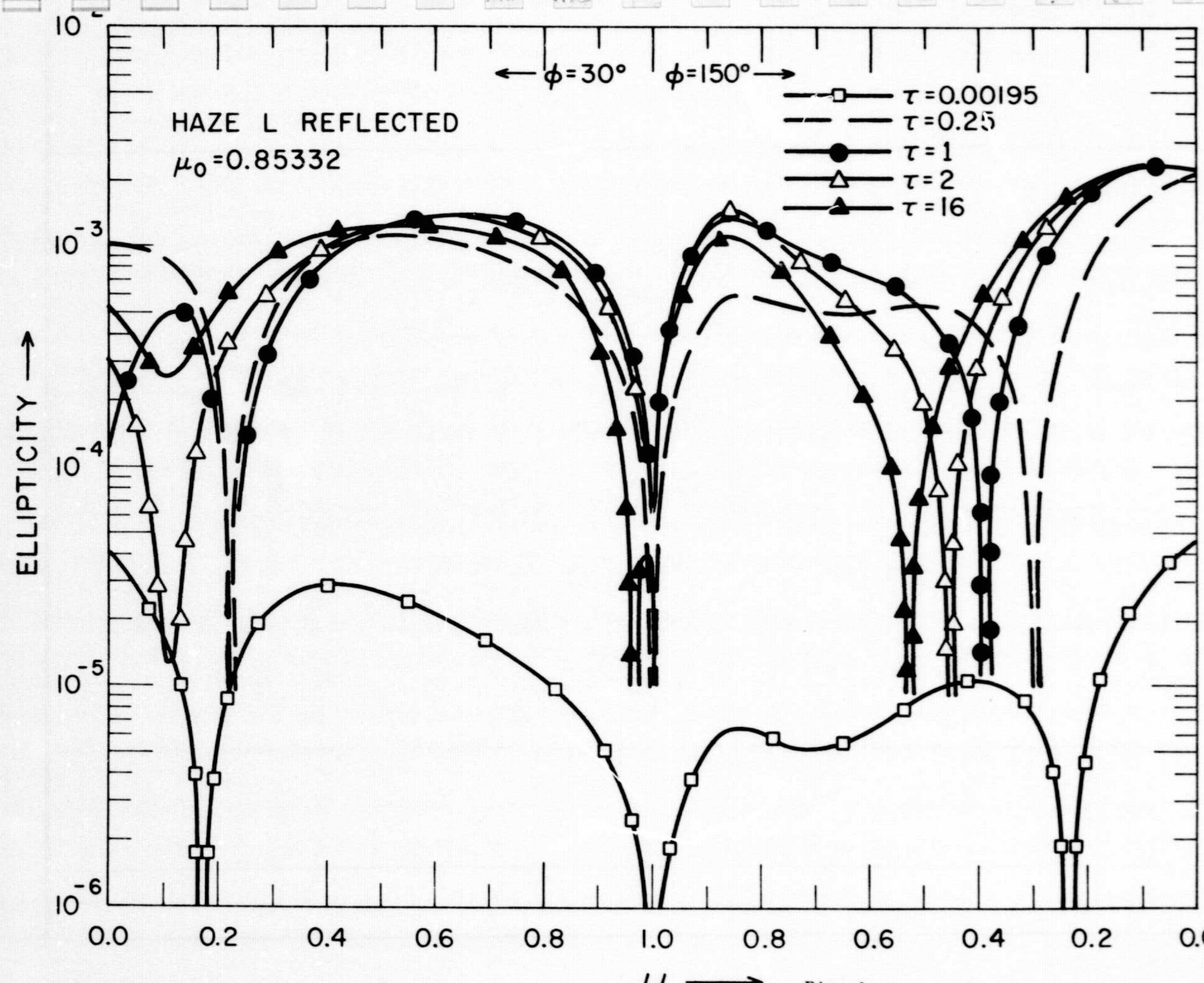
HAZE L REFLECTED
μ_0=0.85332
← ϕ=30°
ϕ=150° →
τ=0.00195
τ=0.25
τ=1
τ=2
τ=16
ELLIPTICITY →
μ →
10^{-2}
10^{-3}
10^{-4}
10^{-5}
10^{-6}
0.0
0.2
0.4
0.6
0.8
1.0
0.8
0.6
0.4
0.2
0.0

Fig. 6

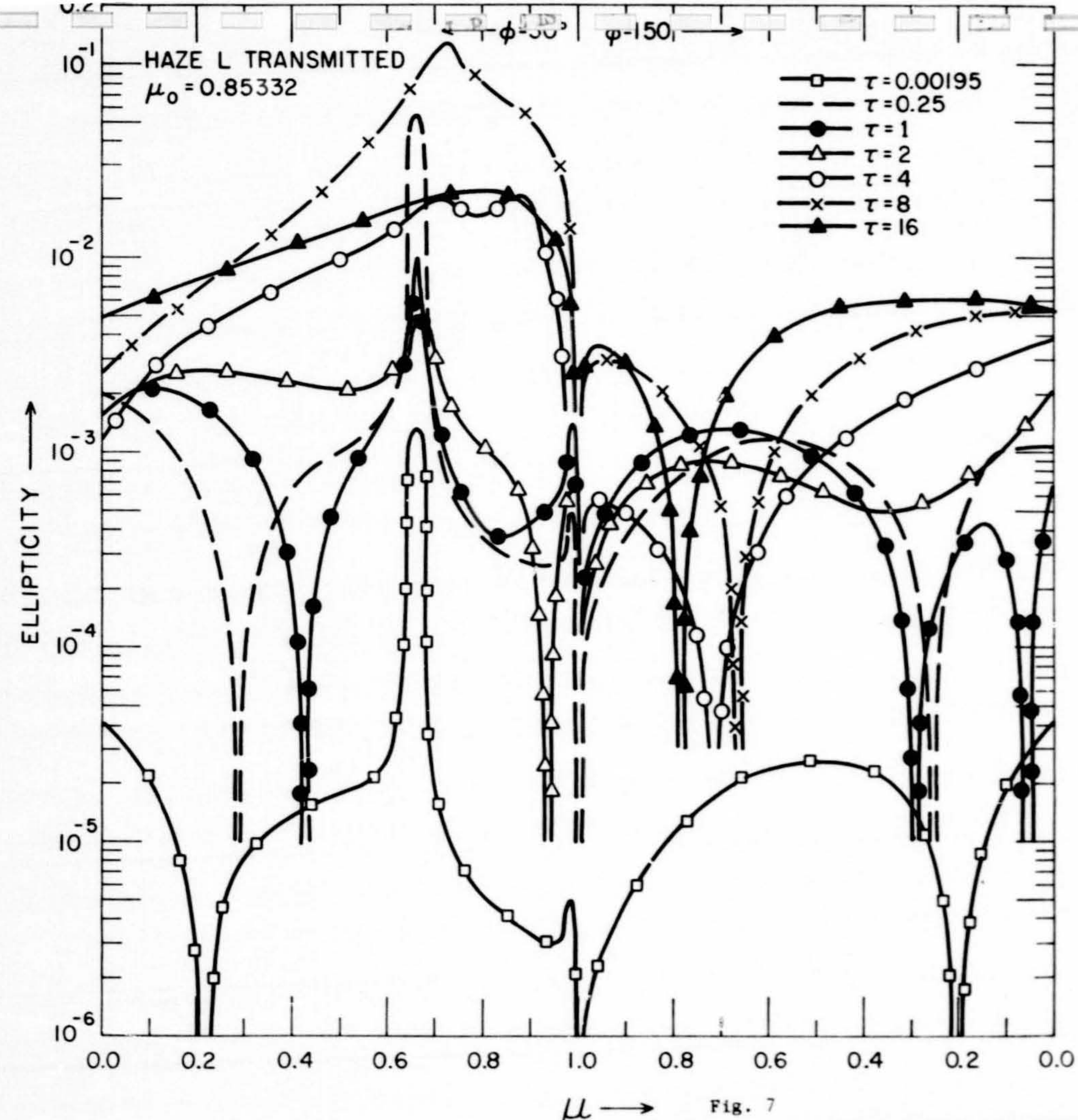

HAZE L TRANSMITTED
$\mu_0 = 0.85332$
$\phi = 30°$
$\phi = 150$
$\tau = 0.00195$
$\tau = 0.25$
$\tau = 1$
$\tau = 2$
$\tau = 4$
$\tau = 8$
$\tau = 16$
ELLIPTICITY
μ

Fig. 7

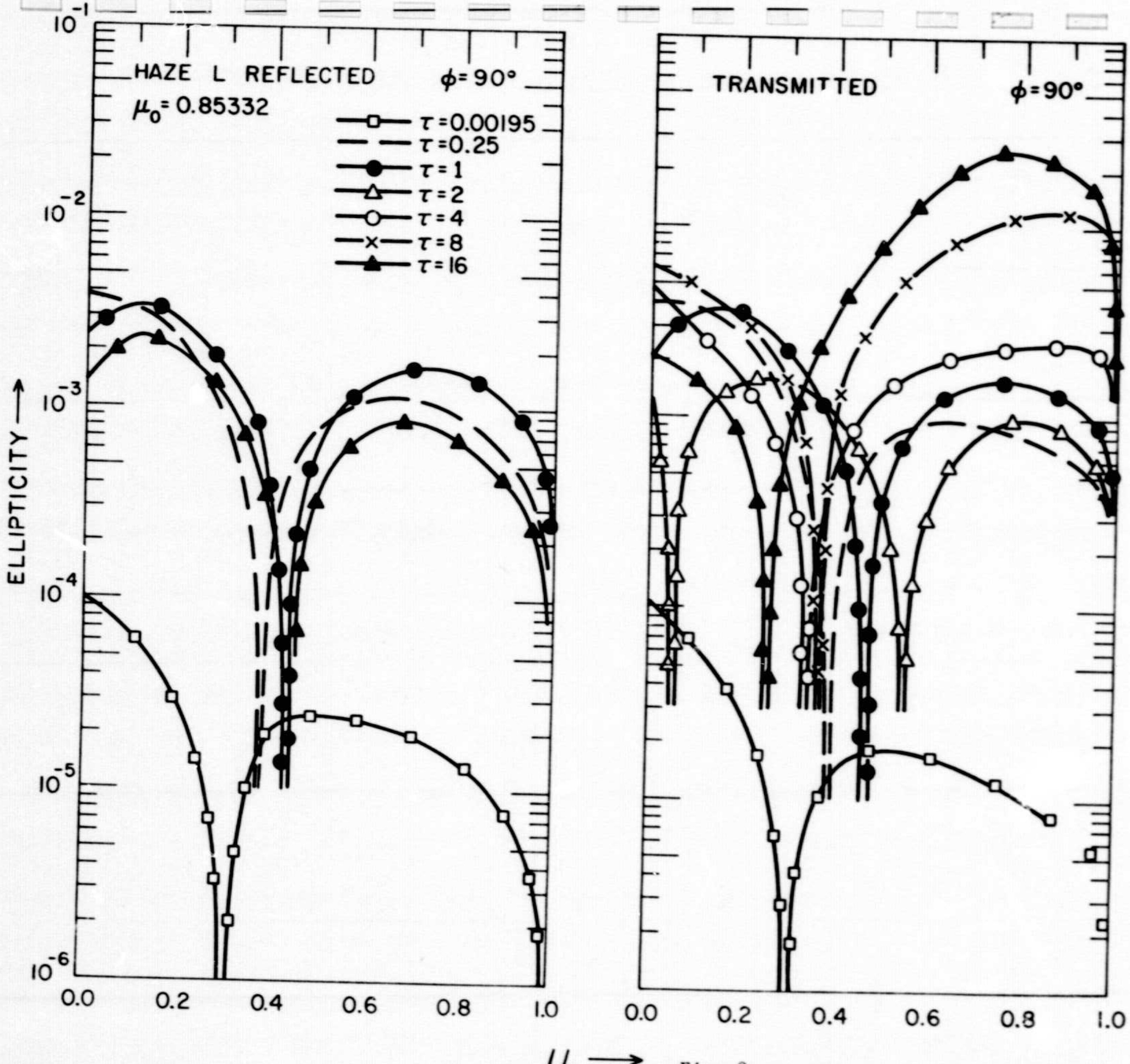
HAZE L REFLECTED
$\phi = 90°$
$\mu_0 = 0.85332$
$\tau = 0.00195$
$\tau = 0.25$
$\tau = 1$
$\tau = 2$
$\tau = 4$
$\tau = 8$
$\tau = 16$
TRANSMITTED
$\phi = 90°$
ELLIPTICITY →
10^{-1}
10^{-2}
10^{-3}
10^{-4}
10^{-5}
10^{-6}
0.0
0.2
0.4
0.6
0.8
1.0
μ →

Fig. 8

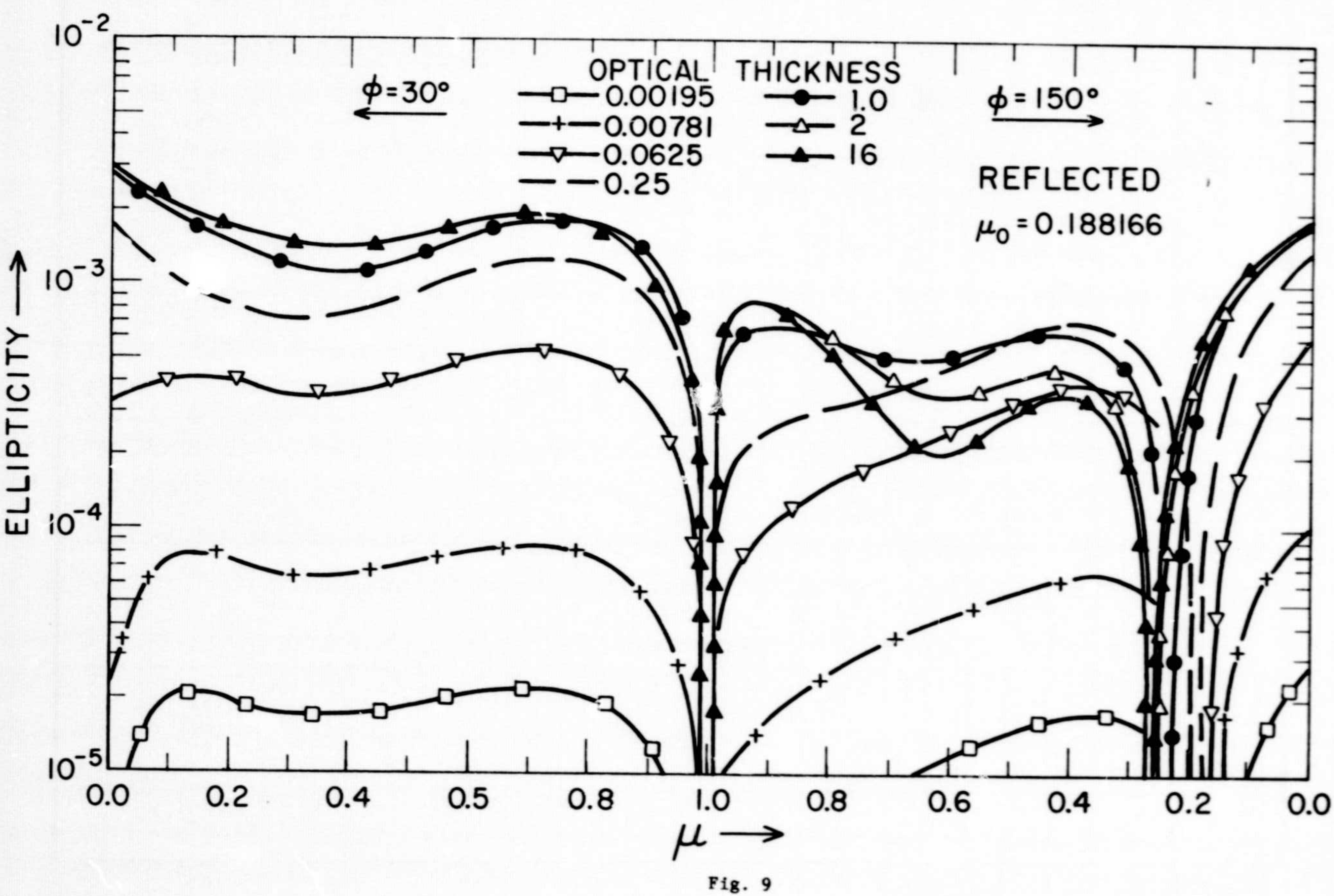

OPTICAL THICKNESS
0.00195
0.00781
0.0625
0.25
1.0
2
16
$\phi = 30°$
$\phi = 150°$
REFLECTED
$\mu_0 = 0.188166$
ELLIPTICITY
10^{-2}
10^{-3}
10^{-4}
10^{-5}
0.0
0.2
0.4
0.5
0.8
1.0
0.8
0.6
0.4
0.2
0.0
μ

Fig. 9

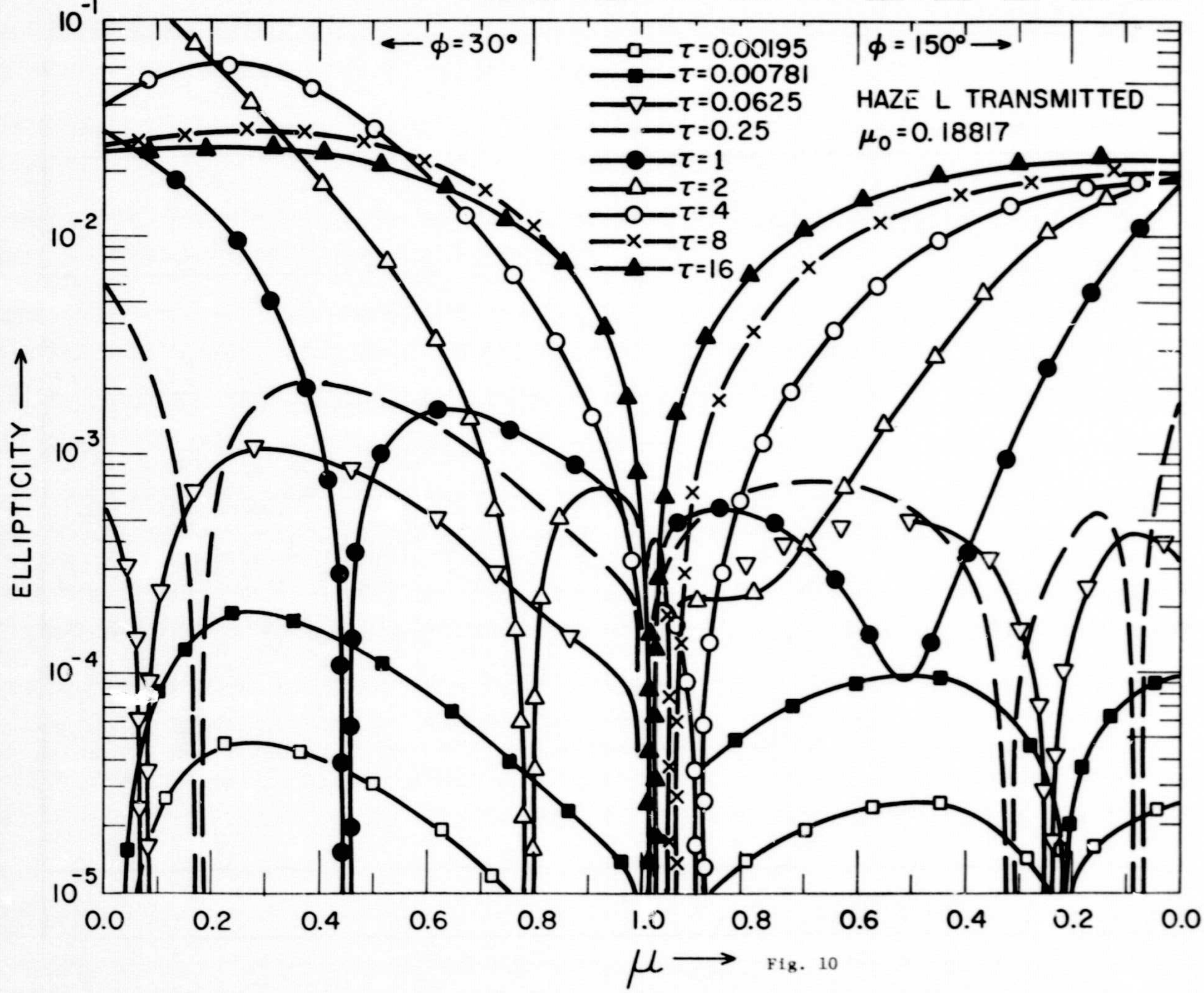

← φ = 30°
φ = 150° →
τ=0.00195
τ=0.00781
τ=0.0625
τ=0.25
τ=1
τ=2
τ=4
τ=8
τ=16
HAZE L TRANSMITTED
μ_0=0.18817
ELLIPTICITY →
10^{-1}
10^{-2}
10^{-3}
10^{-4}
10^{-5}
0.0 0.2 0.4 0.6 0.8 1.0 0.8 0.6 0.4 0.2 0.0
μ →

Fig. 10

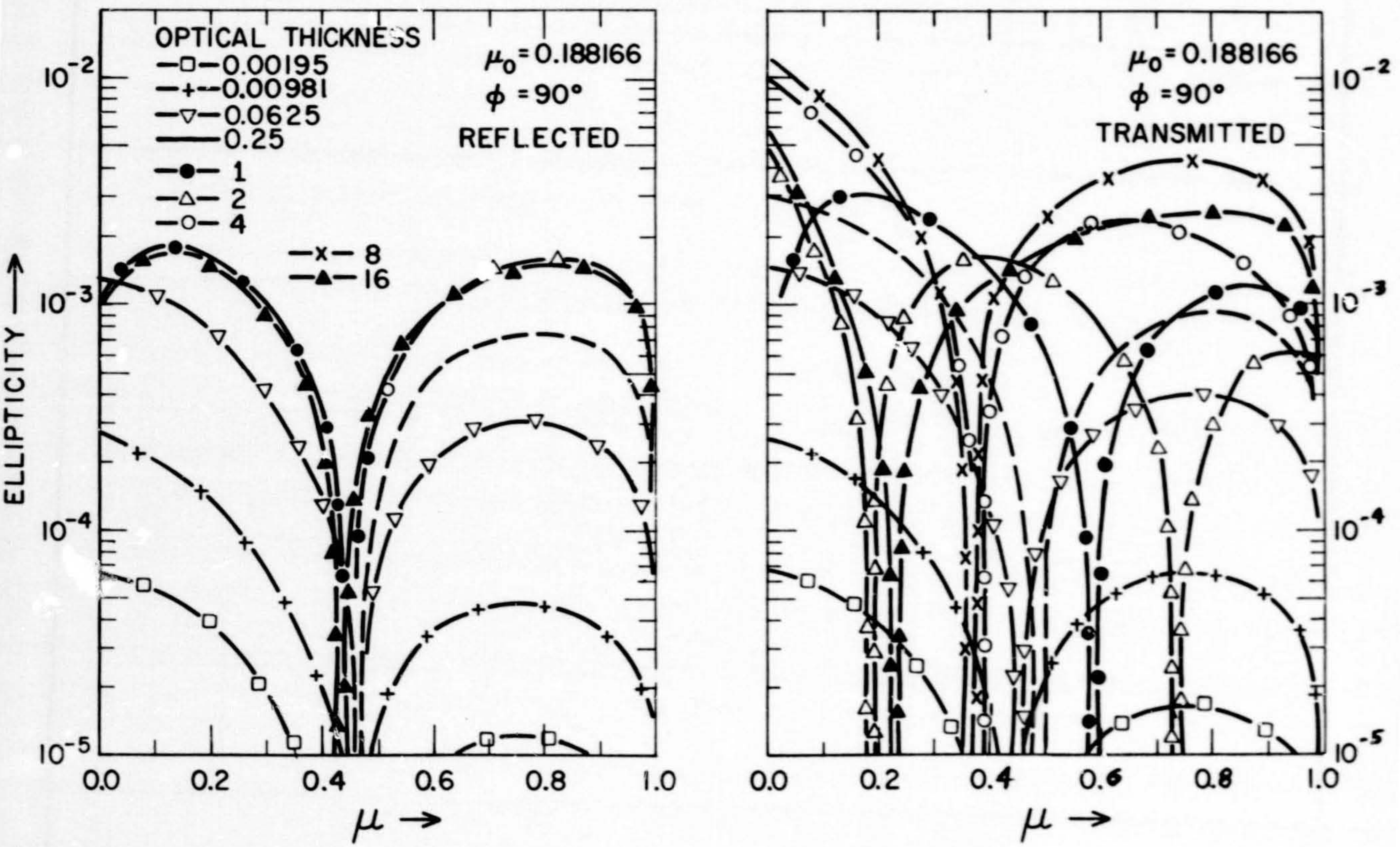
OPTICAL THICKNESS
0.00195
0.00981
0.0625
0.25
1
2
4
8
16
μ_0 = 0.188166
ϕ = 90°
REFLECTED
TRANSMITTED
ELLIPTICITY →
μ →
10^{-2}
10^{-3}
10^{-4}
10^{-5}
0.0
0.2
0.4
0.6
0.8
1.0

Fig. 11